Journal of CO2 Utilization 68 (2023) 102369

Contents lists available at ScienceDirect

Journal of CO2 Utilization

journal homepage: www.elsevier.com/locate/jcou

Hydrothermal reduction of CO_2 captured as $NaHCO_3$ into formate with metal reductants and catalysts

Laura Quintana-Gómez [a], Pablo Martínez-Álvarez [a], José J. Segovia [b], Ángel Martín [a,*], M. Dolores Bermejo [a]

[a] BioEcoUva. Research Institute on Bioeconomy, PressTech Group, Department of Chemical Engineering and Environmental Technology, Universidad de Valladolid, Doctor Mergelina s/n, 47011, Valladolid, Spain

[b] BioEcoUva. Research Institute on Bioeconomy, Laboratory of Thermodynamic and Calibration TERMOCAL, Department of Energy and Fluid Mechanics Engineering, Universidad de Valladolid, Paseo de Belén s/n, 47011, Valladolid, Spain

ARTICLE INFO

Keywords:
Hydrothermal CO_2 reduction
Sodium formate
Metal reductant
Pd/C catalyst
Kinetic model

ABSTRACT

The hydrothermal reduction of CO_2 captured in aqueous solutions using metal reductants is a promising novel approach that achieves high yields of conversion and high selectivity, but it presents the limitation of the high temperatures needed for the reaction to take place. In this work, experiments combining several reductant metals (Zn, Al and Fe), catalysts (Pd/C, Ni, Cu, Fe_2O_3 and Fe_3O_4) and temperatures (200, 250 and 300 °C) were performed to optimize the process at milder temperatures. Using Al as reductant and Pd/C as catalyst, yields as high as 38 % were obtained at 200ºC, compared with the highest yield (57 %) observed at 250 ºC. Thus a significant temperature reduction can be achieved using a suitable combination of reductant and catalyst. Using this reaction system, Pd/C as catalyst and Al as reductant, an extensive set of experiments at different times and temperatures were performed in order to determine the kinetics of the process and correlate them to a mathematical model of the process. The model correctly reproduces the experimental data with average errors lower than 5.9 %. These results demonstrate the feasibility of lower the operating temperature while maintaining the performance, when using an adequate combination of catalyst and reductant.

1. Introduction

Extensive use of fossil fuels along has conducted to a rapid and continuous increase of CO_2 concentration in the atmosphere [1], up to 420 ppm in April 2022, while preindustrial levels were of 278 ppm (in ca. 1750) [2]. Therefore, there is an increasing interest in CO_2 capture and conversion processes that can contribute to revert this trend.

CO_2 capture consists of selectively removing the CO_2 from ambient air or industrial process streams to produce a concentrated stream of CO_2 that can be transported to the storage site [3]. Among the technologies developed for CO_2 capture, chemical and physical absorption stand out, since they are the most mature and used at commercial scale [4]. Usually, CO_2 is absorbed by aqueous solutions of amines or NaOH [5,6]. However, CO_2 capture and storage presents high costs due to the desorption and compression steps prior to transportation [5]. The utilization of this captured CO_2 to produce value-added chemicals may compensate the costs associated to its capture [7]. Nevertheless, the industrial use of CO_2 as a raw material is still limited due to its high chemical stability [8].

There are different alternatives to produce chemicals and fuels from CO_2, including hydrogenation [9], electrochemical reactions [10] and photochemical reactions [11]. However, these technologies still show low yields and high cost and, therefore, further development is necessary [12]. Hydrogen is the main reductant used in these processes. Although nowadays most of the hydrogen is still produced by energy intensive processes, such as the endothermic steam methane reforming (SMR) [13], it is expected that in the near future abundant green hydrogen, produced by water hydrolysis, will be available, since pilot to commercial-scale plants are rapidly developing [14]. In-situ hydrogen production methods that can yield a more reactive reductant at a lower cost also are of high interest.

High-temperature water (HTW) has emerged as an alternative hydrogen donor and reaction media due to the fact that it presents fewer and weaker hydrogen bonds, lower dielectric constant and a higher isothermal compressibility than water at room temperature. Moreover, its use is preferred over organic solvents because it is an environmentally

* Corresponding author.
E-mail address: mamaan@iq.uva.es (Á. Martín).

https://doi.org/10.1016/j.jcou.2022.102369
Received 23 September 2022; Received in revised form 11 November 2022; Accepted 9 December 2022
Available online 12 December 2022

friendly solvent [15]. The dissociation of water with a metal under hydrothermal conditions is an alternative to direct use of hydrogen in the reduction of CO_2. Studies on the abiotic synthesis of organics indicate the feasibility of H_2O dissociation and production of organics by CO_2 reduction using metals under hydrothermal conditions [16–18]. The formation of long-chain hydrocarbons by hydrothermal reduction has also been recently demonstrated [19]. Moreover, organics, such as CH_4 [20] and other hydrocarbons [21] have been found in hydrothermal oceanic vents which may indicate the leading role that reactions such as serpentinization of magnesium-and iron-rich rocks to produce H_2 may have had in the origin of life on the Earth.

For the industrial development of this technology, to find an active catalyst for CO_2 conversion under mild conditions is crucial for using CO_2 as a raw material in the production of chemical and fuels. Among other types, such as homogeneous and biological catalysts, heterogeneous catalysts show some advantages such as high stability and easy separation from reactants and products. Thus, they are usually preferred for their use in industrial applications [22].

Different products can be synthesized from CO_2 using metal reductants and catalysts in hydrothermal conditions. For example, CH_4 was produced with a yield of 98 % from $NaHCO_3$ using Raney Ni nanoparticles as catalyst [23], and acetate was obtained with yields in the range of 10 % using cobalt-based catalysts [24]. In addition to CH_4, methanol can also be formed using CO_2 as the raw material [25,26]. The production of formic acid by the reduction of CO_2 captured as $NaHCO_3$ under hydrothermal conditions has been previously studied to optimize the reaction parameters, particularly the reductant:catalyst:$NaHCO_3$ molar ratio, the reaction temperature and time and the amount of water employed. For instance, using a combination of Ni as catalyst and Fe as the reductant with a ratio 1:1, a yield to formic acid of 15.6 % was reached after 2 h of reaction at 300 ºC [27,28]. Higher yields to formic acid of 63.6 % were found when using a combination of Fe and Cu with a molar ratio 6:6:1 of Fe/Cu/$NaHCO_3$ at the same reaction time and temperature [29]. The performance of Fe reductant without catalyst was also investigated, yielding 92 % of formic acid when employing high proportions of Fe [30]. Zn can also be used as reductant for the hydrothermal reduction of $NaHCO_3$, with yields between 64 % and 78 % at 300 and 325 ºC respectively [31,32], values that could be increased with Ni catalysts [33]. In the case of Al, the yield to formic acid obtained after 2 h of reaction at 300 ºC was also 64 % [34]. Besides the high yields obtained in the hydrothermal reduction of CO_2 using metals, it presents solutions to two of the challenges of CO_2 reduction processes presented above: the reactivity of CO_2 captured in basic solutions, such as HCO_3^-, is higher than that of gaseous CO_2, and the reaction can take place in the same aqueous media where CO_2 is captured by NaOH, without intermediate separation or purification processes, thus avoiding the related energy consumption and processing costs.

The main product obtained in most of these studies is formic acid. Formic acid can be used as preservative and insecticide, as a reducing agent, or as carbon source in synthetic chemical industries [35]. The dehydrogenation of formic acid to produce hydrogen is a fast and easily controllable process and therefore, in the past years, formic acid has also gained great attention as a hydrogen storage vector.

The hydrothermal reduction of CO_2 therefore presents promising advantages in terms of integration with capture processes, selectivity and yield, but the harsh pressure and, particularly, temperature conditions required to carry it out still are a concern, since these conditions have a direct impact on the cost of the process and on the stability of the base (e.g. amine) used to capture CO_2 and, therefore, the possibility to recycle it. It is therefore of great interest to reduce the required operating temperature, while maintaining the performance of the process. With this purpose, in this work a large number of combinations of metal reductants and catalysts are tested systematically. In comparison with previous studies, in which tested temperatures were above 250 ºC, in this work operating temperatures are reduced down to 200 ºC. Moreover, a kinetic model under the optimum reaction conditions is provided.

2. Materials and methods

2.1. Materials

$NaHCO_3$ (100 %) was purchased from COFARCAS (Spain). The reductants employed included Zn powder (< 150 μm, 99.995 % metal basis) and Fe powder (≥ 99 %), both provided by Sigma Aldrich (Spain), and granular Al (< 1 mm, 99.7 %) from Panreac (Spain). The catalysts used encompassed Cu powder (<425 μm, 99.5 % metal basis), Ni powder (< 150 μm, 99.99 %), Fe_3O_4 powder (50–100 nm, 97 % metal basis) and Pd/C (5 % Pd content) acquired from Sigma Aldrich (Spain), as well as Fe_2O_3 powder (< 5 μm, ≥ 96 %) from Panreac (Spain). A standard reagent formic acid (puriss. ~98 %) from Sigma Aldrich was used for obtaining the calibration curves. All reductants and catalysts were used without further treatment or purification.

2.2. Experimental procedure

Aqueous solutions of $NaHCO_3$ were used as the CO_2 source. $NaHCO_3$ solutions were prepared with MilliQ water at a concentration of 0.5 M. Experiments were conducted in batch reactors (length: 16 cm, o.d.: ½", wall thickness: 0.083″) made of SS 316 stainless steel tubing with an internal volume of 9 mL.

Each reactor was loaded with the selected reductant in a molar ratio reductant:CO_2 of 5:1 and the catalyst in a molar ratio catalyst:CO_2 of 2:1, except in the case of Pd/C catalyst, were due to limitations with respect to the volume of solids that could be loaded in the reactor while maintaining an efficient stirring, a catalyst:CO_2 mass ratio of 0.25:1, corresponding to a Pd: CO_2 molar ratio of 0.005:1, was used. Thereafter, the reactor was filled with $NaHCO_3$ solution up to approximately 40 % of the volume of the reactor. The closed reactors were placed in an Al_2O_3 sand fluidized heating bed preheated at the target temperature (200, 250 or 300 ºC) to ensure a rapid heating, which required between 3 and 5 min at the temperature range of 200–300 ºC. After the reaction time was completed, reactors were introduced in a cold water bath to quench the reaction. Liquid samples were collected and the solid reductants and catalysts were separated by vacuum filtration and dried at 105 ºC overnight. To ensure reproducibility, each reaction was conducted at least twice and the standard deviation between the results of the repeated experiments was calculated.

2.3. Analysis of the products

Liquid samples were analyzed by HPLC (Waters, Alliance separation module e2695) attached to a RI detector (Waters, 2414 module) using a Rezex-ROA-Organic Acid (8 %, pore size 300 ×7.8 mm) purchased from Phenomenex. Prior to analysis, all the samples were filtered through a 0.22 μm filter. The HPLC method consisted of passing a mobile phase of 25 mM of H_2SO_4 with a flow rate of 0.5 mL/min during 30 min. The temperatures of the column and the detector were set at 40 and 30 ºC, respectively. Each sample was analyzed twice to ensure reproducibility of the HPLC operation.

The yield of formate was calculated according to Eq. 1:

$$Y_{Formate} = \frac{C_{Formate,f}}{C_{NaHCO3,i}} \times 100 \quad (1)$$

where $C_{Formate,f}$ is the molar concentration of formate obtained at the end of the reaction calculated by calibration curves in HPLC analysis, and $C_{NaHCO3,i}$ is the initial concentration of the $NaHCO_3$ aqueous solution, fixed at 0.5 M.

2.4. Solids characterization

XRD patterns were recorded using a Bruker D8 Discover A25 diffractometer attached to a LynxEye detector operated at a voltage of 40 kV and a current of 30 mA. Data were collected at room temperature in the 2θ range from 5 to 70º with a step size of 0.020º using Cu Kα radiation (λ = 1.5418 Å). Database PDF-2-ICDD 2020 was used to analyze the XRD patterns collected.

N_2 gas adsorption was used to determine the surface area of the fresh Pd/C catalyst. The catalyst surface area was measured according to BET method using a ASAP™ 2420 Micromeritics Accelerated Surface Area and Porosimetry System. 0.1133 g of fresh Pd/C was introduced in the sampling tube and after degassing it under vacuum overnight, and the N_2 isotherms were recorded at − 196 ºC.

2.5. Kinetic equations

In a previous work of this research group [35], it was stated that in this type of reactions the equilibrium formic acid/formate is mostly shifted to formate due to the reaction pH, which is alkaline. Therefore, the reactions considered are presented in R1-R4.

$$2H_2O(l) + Al(s) \rightarrow 1.5H_2(aq) + AlO(OH)(s) \quad \text{(R1)}$$

$$NaHCO_3 + H_2 \rightarrow Na^+ + HCOO^- + H_2O \quad \text{(R2)}$$

$$HCOO^-(aq) + H_2O(l) \rightarrow HCO_3^-(aq) + H_2(aq) \quad \text{(R3)}$$

$$HCOO^-(aq) \rightarrow CO(g) + OH^-(aq) \quad \text{(R4)}$$

In this previous work, it was observed that the reaction R1 of production of hydrogen was much faster than bicarbonate reduction [35]. Thus, this first step was not considered in the simplified model, assuming that H_2 is instantaneously formed. With R2, bicarbonate is reduced to formate using hydrogen. This formate is decomposed to CO_2 (R3) and to CO (R4) [36]. As the conversion of the decomposition of $HCOO^-$ to CO (R4) is at least an order of magnitude lower than the conversions of R3, the formation of CO was also not taken into account for simplification purposes [36]. As equilibrium calculation presented in a formed work [35] resulted that most CO_2 was dissolved in aqueous solutions as bicarbonate, in R3 the product is HCO_3^- instead of gaseous CO_2.

Having into account these simplifications, the global reaction taken account in the model is R5, presented as a pseudo-equilibrium reaction.

$$NaHCO_3 + H_2 \leftrightarrow Na^+ + HCOO^- + H_2O \quad \text{(R5)}$$

Whose kinetics follow Eq. 1:

$$\frac{dC_{NaHCO_3}}{dt} = \frac{1}{S_{cat}}\left(-k_1 \bullet C_{NaHCO_3}^m \bullet C_{H_2}^n + k_2 \bullet C_{HCOO^-}^p\right) \quad (1)$$

Where S_{cat} is the surface area of the catalyst, k_1 and k_2 are the kinetic constants of bicarbonate and formate decompositions, direct and inverse reactions, respectively; m, n and p the order of the reaction respect to each compound, C_{NaHCO_3} is the concentration of bicarbonate, C_{HCOO^-} is the concentration of formate and C_{H_2} is the concentration of H_2.

To study the kinetics of the reaction, experiments were conducted at different times, specifically 15, 30, 60, 90 and 120 min. At these times, the concentration of $NaHCO_3$ and $HCOO^-$ were quantified by HPLC analysis. It is important to highlight that the concentration of H_2 (C_{H_2}) is considered constant due to the fact that it is assumed that the metal reductant is completely oxidized and H_2 is released very quickly, according to the results obtained in a previous work [35]. As the mole ratio of reductant to $NaHCO_3$ employed is 5:1, the amount of H_2 formed is highly in excess in comparison to $NaHCO_3$. Moreover, H_2 is present in both gas and liquid phase. The concentration of H_2 in the liquid phase is determined by its solubility at the pressure and temperature of the reaction media. To calculate the solubility of H_2 the next steps were followed:

(1) As aforementioned, it is assumed that the reductant is completely oxidized. Therefore, the amount of H_2 formed depends on the redox reaction of the reductant and water. In the case of Al reductant, 1.5 mol of H_2 is formed per each mol of Al, according to Reaction R1. Considering this, it can be assumed that the concentration of H_2 remains constant during the reaction since the molar ratio H_2:CO_2 is 7.5, and therefore, $NaHCO_3$ is the limiting reactant.
(2) The volume that the H_2 occupies is 5.4 mL, this is, the total volume of the reactor (9 mL) minus the volume of the solution of $NaHCO_3$ added (3.6 mL).
(3) Using the ideal gas equation, the pressure of H_2 is calculated in that volume at the reaction temperature.
(4) Using data generated with the Predictive Soave Redlich Kwong (PSRK) equation [37], a model to calculate the molar fraction of H_2 dissolved in H_2O is developed. The model is valid from pressures from 50 to 150 atm. For simplification of the calculations, the results of this thermodynamic model were correlated according to Eqs. 2–4 for 200, 250 and 300 ºC respectively. Model fit showed a $R^2 = 1.00$,$R^2 = 0.998$ and $R^2 = 0.988$ for the temperatures 200, 250 and 300 ºC respectively.

$$x_{H2} = 5.834 \bullet 10^{-8}P^2 + 2.004 \bullet 10^{-5}P - 3.0689 \bullet 10^{-4} \quad (2)$$

$$x_{H2} = 2.375 \bullet 10^{-7}P^2 - 1.084 \bullet 10^{-5}P + 1.154 \bullet 10^{-3} \quad (3)$$

$$x_{H2} = 5.748 \bullet 10^{-7}P^2 - 7.5346 \bullet 10^{-5}P + 2.906 \bullet 10^{-3} \quad (4)$$

where x_{H2} is the molar fraction of H_2 in H_2O and P the pressure in atm.
(5) The number of mole of H_2O at reaction conditions is calculated taken into the account its density at the reaction temperature and pressure. The density of the H_2O was calculated with the MS Excel Add-In Water97v13.xla [38].
(6) The solubility of H_2, and thus, the amount of H_2 in water, can be calculated using the model developed in step 4 and the amount of H_2O calculated in step 5.
(7) Once the amount of H_2 in H_2O is known, the H_2 remaining in the gas phase is recalculated.
(8) With this new value of the H_2 in gas phase, its pressure is calculated according to step 3. Steps 4, 5, 6 and 7 are iterated until the pressure calculated in step 7 converges to the one used in step 3.
(9) Once the values of the H_2 pressure calculated in steps 3 and 7 are equal, the amount of H_2 in H_2O is given by steps 4 and 5.

Once the initial concentrations of $NaHCO_3$, H_2 and $HCOO^-$ are known, the system is modeled considered it as a discontinuous stirred tank reactor, solving the mass balances to formic acid, hydrogen and bicarbonate. In addition to Eq. 1, Eqs. 5 and 6 were also solved, using the Euler numerical method:

$$C_{NaHCO3}(t) = C_{NaHCO3}(t-1) + \frac{dC_{NaHCO3}(t-1)}{dt} \bullet dt \quad (5)$$

$$C_{HCOO^-}(t) = C_{HCOO^-}(t-1) - \frac{dC_{HCOO^-}(t-1)}{dt} \bullet dt \quad (6)$$

(1) The differential equations are solved using the Euler method with a time step of 10 s. The values of the orders of the reaction, this is m, n and p simulated were 1, 2 and 0.5. All the combinations of these values were simulated in order to optimize.
(2) With the fixed reactions orders, the values k_1 and k_2 were optimized in order to minimize the objective Eq. 7 using the function Solver of Excel:

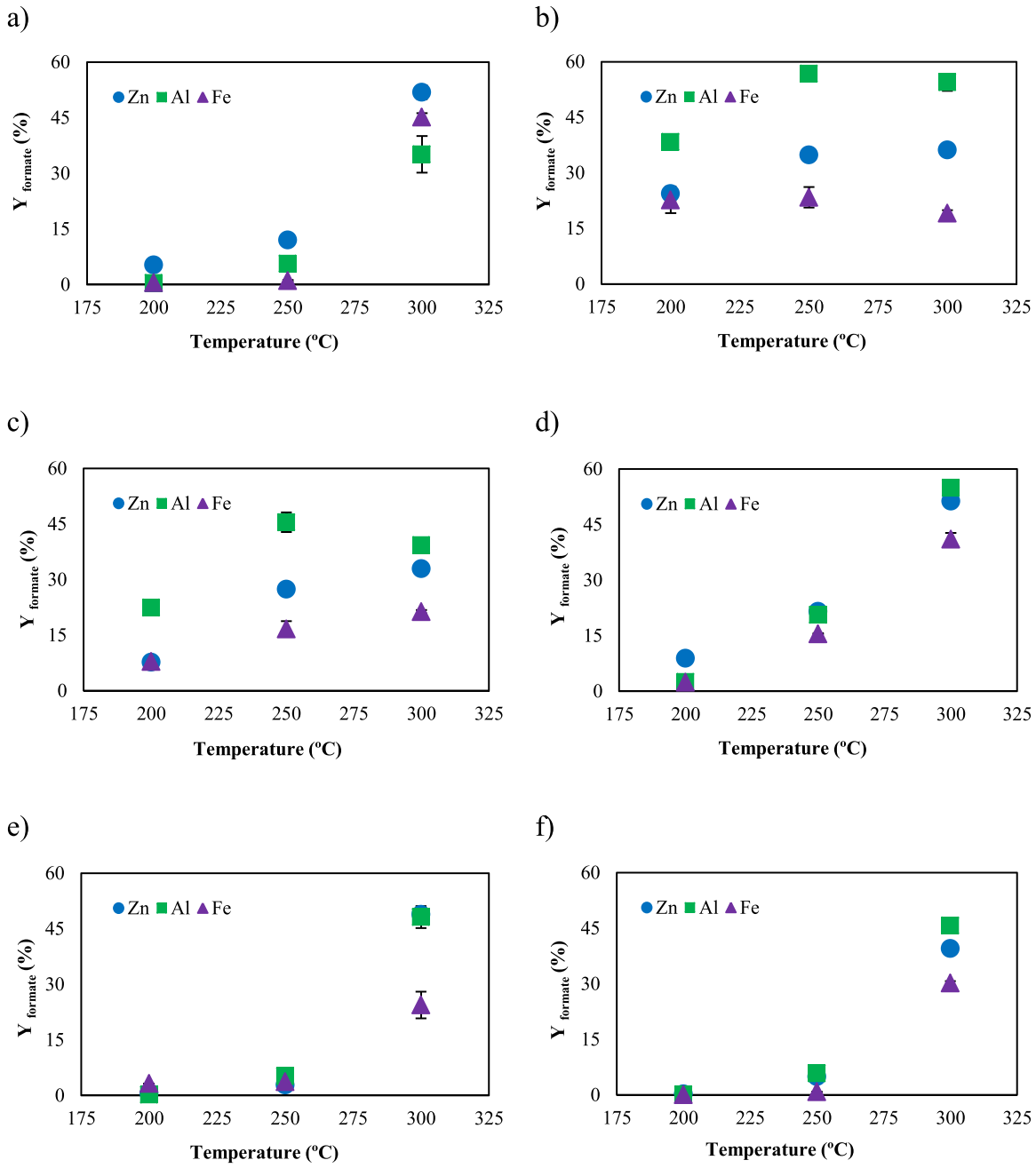

Fig. 1. Formate yields with different reductants at temperatures from 200–300 ºC. a) without catalyst; b) Pd/C catalyst; c) Ni catalyst; d) Cu catalyst; e) Fe_2O_3 catalyst and f) Fe_3O_4 catalyst. Reaction conditions: reactor filling: 40 %, reductant:CO_2 mole ratio: 5, catalyst:CO_2 mole ratio: 2 except in Pd/C where 0.018 g of catalyst were used and reaction time: 120 min.

$$AVERAGE \sum_{t=15\text{min}}^{t=120\text{min}} ABS\left(\frac{C_{NaHCO3\_MODEL} - C_{NaHCO3\_EXPERIMENTAL}}{C_{NaHCO3\_EXPERIMENTAL}}\right) = 0 \quad (7)$$

where $C_{NaHCO3\_}$ is the concentrration of $NaHCO_3$ obtained with the model and $C_{NaHCO3\_}$ is the value of $NaHCO_3$ experimentally obtained.

(3) The combination of reaction orders selected was the one where the sum of the average absolute error for the concentration of $NaHCO_3$ plus the average absolute error of the concentration of formate was smaller.

The kinetic constants were correlated at three different temperatures: 200, 250 and 300 ºC. The values of the constant were adjusted to Arrhenius equation to easily calculate the effect of the temperature (Eq. 8).

$$k(T) = A \bullet e^{-\frac{E_a}{RT}} \quad (8)$$

where $k(T)$ is the rate constant as a function of the temperature, A is the pre-exponential factor, E_a the activation energy, R is the gas constant and T is the absolute the reaction temperature.

3. Results and discussion

3.1. Production of formate

This work studied the influence of different combinations of

Table 1
Formate yields with different metal reductants, catalysts and reaction temperatures.

		Temperature		
Reductant	Catalyst	200ºC	250ºC	300ºC
Zn	–	5.4 ± 0.9	12.0 ± 0.7	51.9 ± 1.9
	Pd/C	24.4 ± 1.9	34.8 ± 0.2	36.2 ± 0.8
	Ni	7.7 ± 1.1	27.4 ± 0.7	33.0 ± 0.1
	Cu	8.9 ± 1.6	21.5 ± 0.3	51.3 ± 1.1
	Fe2O3	0.5 ± 0.1	2.8 ± 0.8	48.9 ± 0.8
	Fe3O4	0.28 ± 0.01	4.9 ± 0.4	39.5 ± 0.1
Al	–	0.4 ± 0.2	5.6 ± 0.3	35 ± 5
	Pd/C	30 ± 1	56.8 ± 1.1	54.5 ± 2.3
	Ni	22.4 ± 1.4	45 ± 3	39.3 ± 0.1
	Cu	2.512 ± 0.004	20.6 ± 0.3	55 ± 2
	Fe2O3	0.223 ± 0.002	5.2 ± 0.4	48 ± 3
	Fe3O4	0.07 ± 0.06	6 ± 2	45.7 ± 1.2
Fe	–	0.5 ± 0.2	1 ± 0.2	45.2 ± 1.1
	Pd/C	23 ± 4	23 ± 3	19.1 ± 0.8
	Ni	7.9 ± 1	17 ± 2	21.3 ± 0.4
	Cu	2.4 ± 0.3	15.50 ± 0.14	41.0 ± 1.7
	Fe2O3	3.230	3.68 ± 0.01	24.4 ± 3.6
	Fe3O4	0.200	0.78 ± 0.07	30.2 ± 0.5

reductants and catalysts to reduce CO_2 to formate under hydrothermal conditions. As aforementioned, $NaHCO_3$ was used as the carbon source, being it the product resulting from the capture of CO_2 with basic NaOH solutions. The reductants employed included Zn, Al, and Fe and the catalysts were Cu, Ni, Fe_2O_3, Fe_3O_4 and Pd/C. Three different reaction temperatures were also explored, specifically 200, 250 and 300 ºC. Temperatures above 300 ºC were not tested since the decomposition of formic acid into CO_2 and H_2 at high temperatures under hydrothermal conditions is high [36].

When using Al or Zn as reductants, the selectivity of liquid-phase products towards formate was 100 %. In the case of using iron as reductant, a peak corresponding to another unidentified product was found apart form the peak of formate. Sample chromatograms are provided as Supplementary Information (Fig. S1). Formate yields are plotted in Fig. 1 together with the error bars calculated from the results of repeated experiments. The standard deviation of the two replicates was lower than 1.5 % in most of the cases and, therefore, some of the error bars cannot be appreciated in Fig. 1 due to the axis scale. Table 1 compiles the yields obtained with the different combinations of metal reductants, catalysts and temperature.

It is clear from Fig. 1 that the temperature has a positive effect on the yield to formate. The higher the temperature, the higher the yield and, in general, the change observed in the yield is greater from 250 to 300 ºC than from 200 to 250 ºC, except in the case of Pd/C and Ni catalysts (Fig. 1b a 1c respectively), where the yield at 300 ºC was only slightly higher than that at 250 ºC when using Zn as the reductant. In contrast, with Al and Fe reductants, the yield to formate decreased moderately from 250 to 300 ºC.

The highest formate yield reached a value of 57 %. It was observed at 250 ºC when the reductant was Al and the catalyst Pd/C. A similar yield of 55 % was obtained at 300 ºC with Cu catalyst, again with Al reductant. Interestingly, a comparable yield of 52 % was detected at 300 ºC with Zn reductant in the absence of catalyst. Indeed, in the absence of catalyst, Zn showed the best performance at the three temperatures evaluated, yielding 5.4 % and 12 % of formate at 200 and 250ºC respectively. In contrast, at 200 ºC, the yields obtained with Al and Fe and without

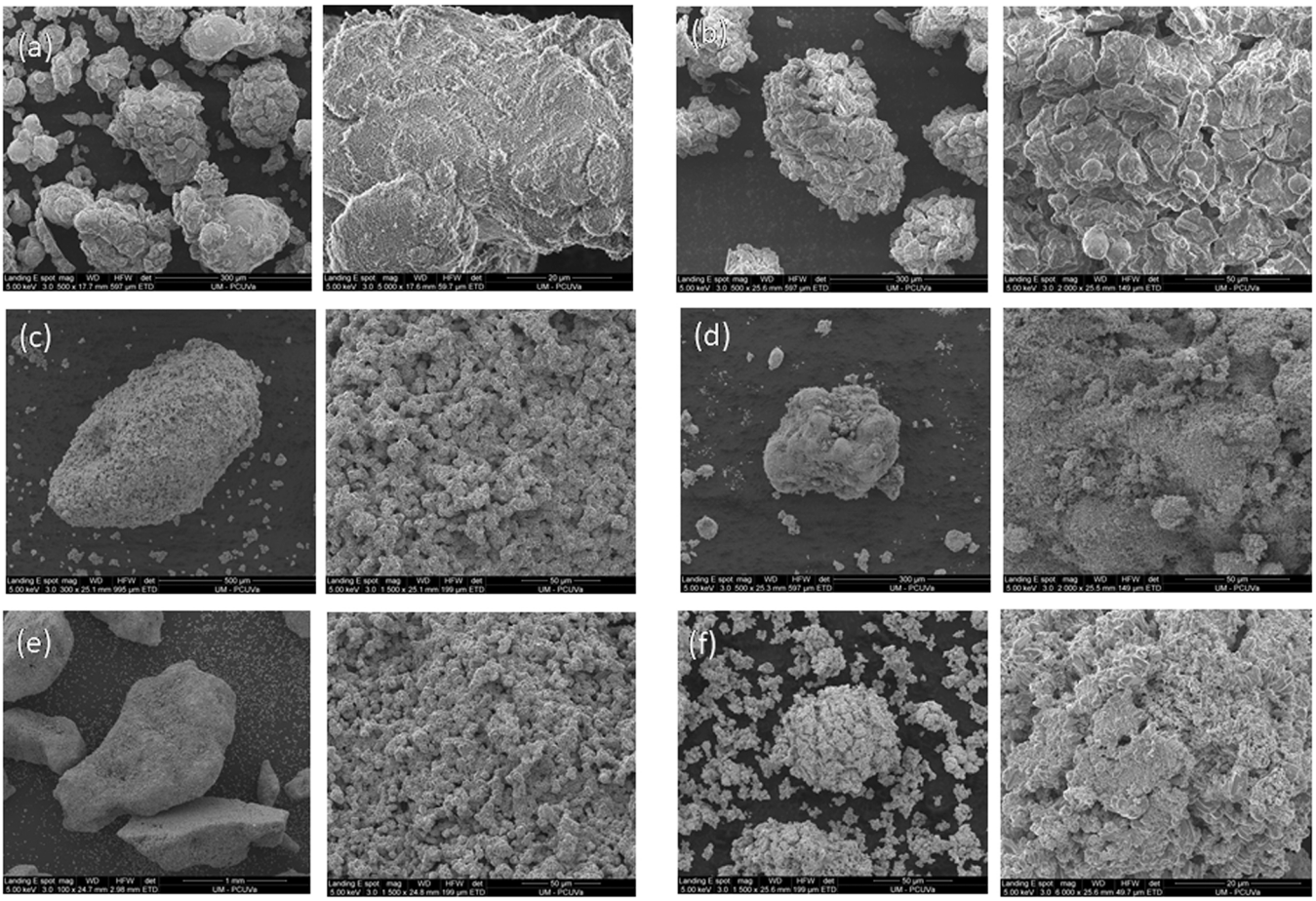

Fig. 2. SEM micrographs of solid samples after reaction experiments. (a) Al as reductant, (b) Al as reductant and Pd/C as catalyst, (c) Fe as reductant, (d) Fe as reductant and Fe_3O_4 as catalyst, (e) Fe as reductant and Fe_2O_3 as catalyst, (f) Zn as reductant.

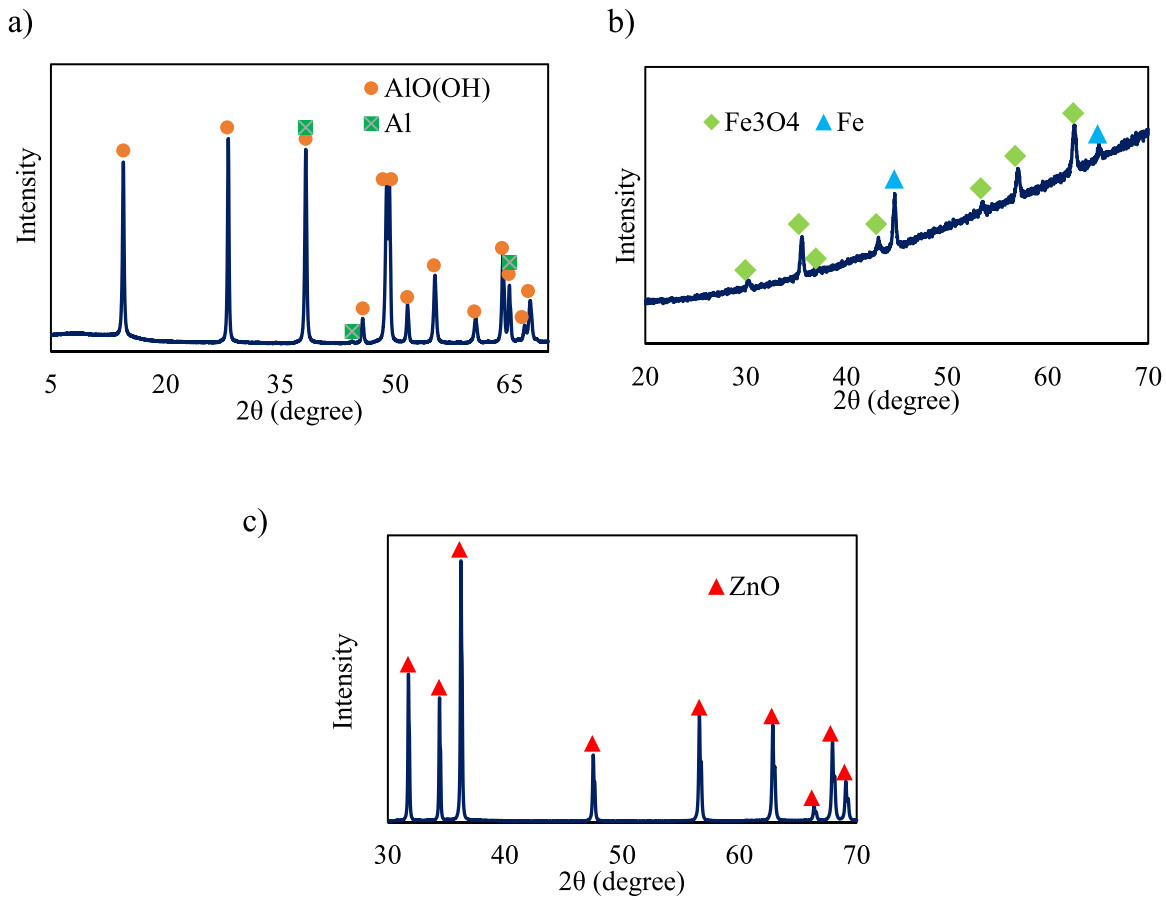

Fig. 3. XRD patterns obtained for the three reductants employed in the absence of catalyst after the hydrothermal reaction of $NaHCO_3$. Reaction conditions: reactor filling: 40 %, reductant:CO_2 mole ratio: 5, temperature: 300 ºC and reaction time: 120 min a) Al reductant; b) Fe reductant and c) Zn reductant.

catalyst were negligible and at 250 ºC the yield with Al was of 5.6 % while in the case of Fe was only 1 %. The feasibility of using Zn reductant to produce formic acid from $NaHCO_3$ under hydrothermal conditions was previously demonstrated [32], where the intermediate Zn-H, obtained by the oxidation of Zn by HTW, may have a leading role by acting as the active hydrogen source in CO_2 hydrogenation [39].

With Fe reductant, the performance of Fe_2O_3 catalyst at 200 and 250 ºC is practically constant, yielding 3 % and 4 % of formate, respectively. The same trend can be observed with Fe_3O_4 catalyst, where the yield at both temperatures was lower than 1 %. However, at 300 ºC, Fe_3O_4 showed a better performance than Fe_2O_3 catalyst for Fe reductant yielding 30 % of formate, while the yield with Fe_2O_3 was 24 %. In general, in the temperature range studied, Fe reductant showed the lowest yields, while Al reductant exhibited the best performance. However, in the absence of catalyst with Fe reductant at 300 ºC, the yield obtained was higher than in the case of Al powder reductant, reaching a value of 45 %. This yield is comparable to that observed by Duo et al. [30], who determined a yield of approximately 50 % with Fe, although they used a low $NaHCO_3$ concentration of 2 mmol/L. Duo et al. [30] significantly increased the yield of formic acid to more than 90 % by increasing the amount of Fe powder employed. The best performance of Fe reductant detected by Duo et al. [30] can be explained by the particle

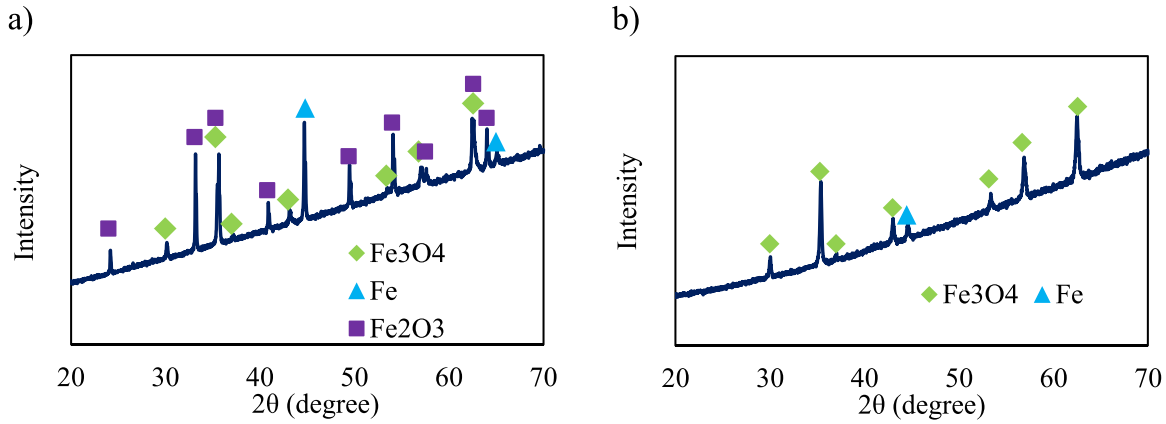

Fig. 4. XRD patterns obtained for Fe reductant and different catalysts in the hydrothermal reaction of $NaHCO_3$. Reaction conditions: reactor filling: 40 %, reductant: CO_2 mole ratio: 5, catalyst:CO_2 mole ratio: 2, temperature: 300 ºC and reaction time: 120 min a) Fe_2O_3 catalyst and b) Fe_3O_4 catalyst.

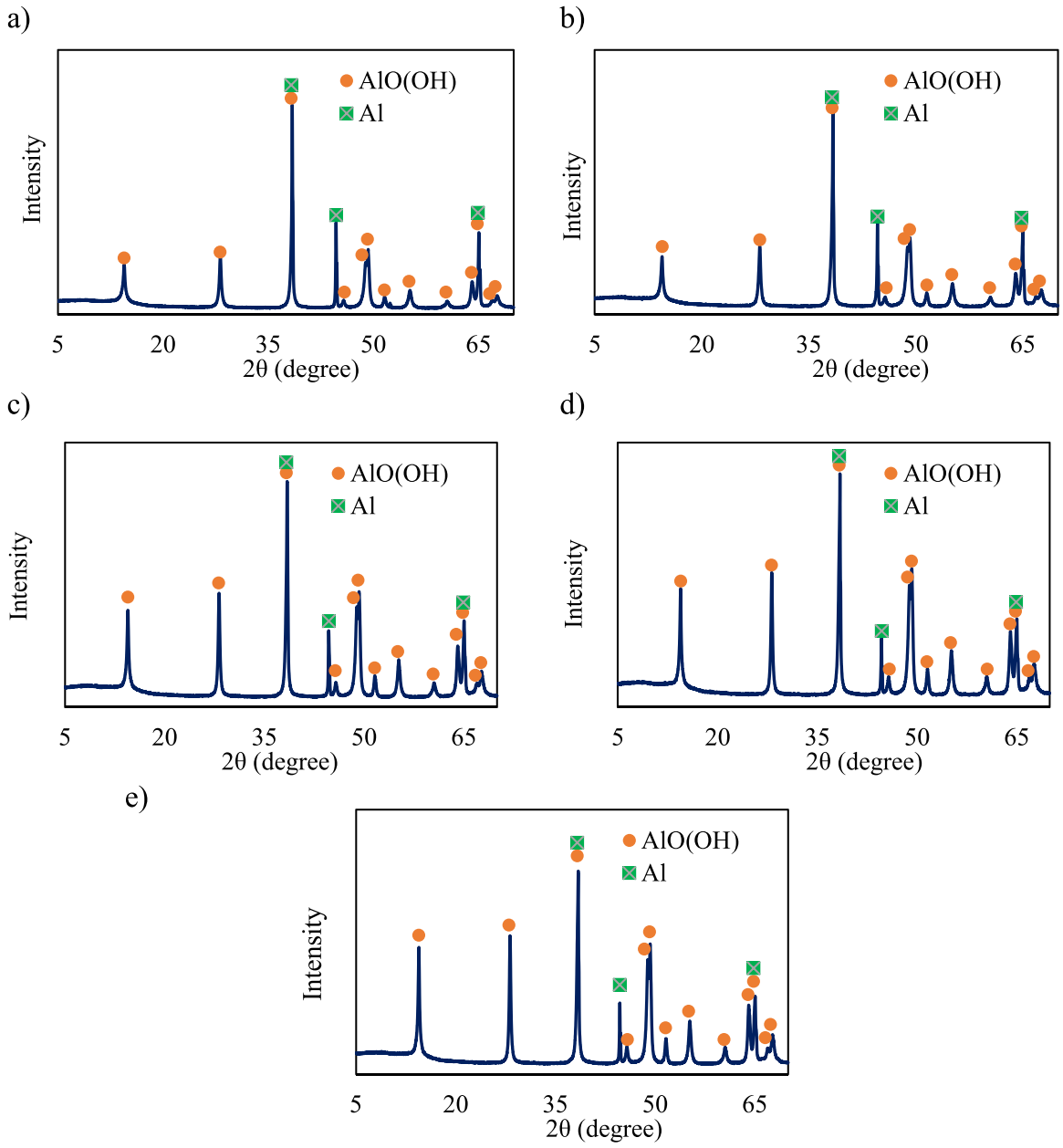

Fig. 5. XRD patterns obtained after the hydrothermal reaction of $NaHCO_3$ using Al as reductant and Pd/C as catalyst at different times. Reaction conditions: reactor filling: 40 %, reductant:CO_2 mole ratio: 5, catalyst:CO_2 mole ratio: 2 and temperature: 300 °C. a) 15 min, b) 30 min, c) 60 min, d) 90 min and e) 120 min.

size of the reductant and the more diluted reaction conditions, along with the horizontally shaken of the reactor which may have enhanced mixing and heat transfer, favoring the reaction. However, for practical applications, higher reactant concentrations are desirable to increase throughput.

It is very well-known that Cu catalyst is very selective to methanol when reacting with CO_2 [25]. However, methanol was not observed in this work, probably due to the alkaline pH of the reaction media, since Huo et al. [25] used HCl to acidify the media to produce methanol.

3.2. Catalyst characterization

Fig. 2 presents SEM micrographs of selected solid samples after reaction experiments, while Figs. 3–5 presents the corresponding XRD patterns. XRD was employed to investigate changes in the phases present in both the reductants and selected catalysts after reaction. Fig. 3 shows the changes in the phases of the three reductants employed after 120 min of reaction at 300 °C. Reference diffractograms of the original, unoxidized metals can be retrieved from [40].

As it is clear from Fig. 3, the only reductant completely oxidized after reacting during 120 min at 300 °C was Zn. This result is in agreement with the works of Jin et al. and Roman-Gonzalez et al. [32,34] who demonstrated that under hydrothermal conditions, Zn was almost completely oxidized to ZnO after 10 min of reaction time. In the case of Al reductant, both crystal phases are present, Al and AlO(OH). However, Yao et al. [33] concluded that the oxidation of Al under hydrothermal conditions in the presence on $NaHCO_3$ was completed after 30 and 90 min of reaction time. This disagreement in the results may be explained by the different particle size of Al powder employed. In Fig. 2b it is shown that Fe was oxidized to Fe_3O_4 under the reaction conditions, but not completely, since typical peaks of Fe crystal phases, specifically at 2θ of 44.8 and 65°, are still present.

XRD analysis of Fe reductant combined with Fe_2O_3 and Fe_3O_4 catalysts was also conducted. The XRD patterns obtained are shown in Fig. 4.

Table 2
Average and maximum error between the experimental data and the model prediction for both bicarbonate and formate.

T (°C)	Average/max. error $NaHCO_3$	Average/max. error formate
200	1.5 % / 3.7 %	5.9 % / 8.5 %
250	2.3 % / 5.8 %	5.1 % / 9.1 %
300	3.6 % / 3.5 %	4.9 % / 6.4 %

It can be seen in Fig. 4 that Fe_2O_3 is only present when it was used as catalyst (Fig. 4a) and therefore, under reaction conditions Fe reductant is only oxidized to Fe_3O_4 (Fig. 4b). The same conclusion can be reached by looking at Fig. 2b. Duo et al. [30] also stated that under hydrothermal conditions, Fe may oxidized to Fe_3O_4 rather than Fe_2O_3. Interestingly, it seems that the presence of Fe_3O_4 in the media promotes in some extent the oxidation of Fe, because after reaction only one a small characteristic peak of Fe phase appeared at 44.5° (Fig. 4b), while in the case of using Fe_2O_3 as catalyst (Fig. 4a) or just Fe as reductant (Fig. 3b), two characteristic phase peaks of Fe are detected, specifically at 44.5° and 65° and with high intensities.

The evolution of the crystal phases of Pd/C catalyst and Al reductant at different reaction times was also investigated. The results are shown in Fig. 4. The XRD patterns at different times shown no apparent differences, as can be seen from Fig. 5. No matter long or short reaction times, Al reductant was not completely oxidized and typical Al crystal phase at 2θ of 38°, 44° and 65° are still detected after 120 min of reaction time at 300 °C. On the other hand, Pd crystal phase could not be detected in the diffractogram, as a consequence of the low concentration of Pd in the Pd/C catalyst (5 %wt) and the low proportion of the catalyst in the total sample (0.018 g of catalyst vs 0.24 g of Al).

3.3. Kinetics

The kinetic behavior of the reaction was investigated at three different temperatures according to the method explained in Section 2.5. The best adjustment to the experimental data at 250 °C and 300 °C was for a first order reaction respect to all components. Therefore, the units of the kinetic constants obtained are expressed in $m^{-2}s^{-1}$. Figures from 5 to 7 show the model for a pseudo-first order reaction respect to all components and the experimental data for temperatures of 200, 250 and 300 °C respectively, while Table 2 presents the average and maximum deviations between experiments and calculations (Eq. 7) obtained at each temperature.

As it can be seen from Figs. 6 to 8, the model correctly describes the experimental results at the three tested temperatures, with average deviations in the concentration of $NaHCO_3$ ranging from 1.5 % to 3.6 %, slightly increasing with temperature. At 250 °C it appears that the experimental point at 120 min differs significantly from the model prediction. Errors in the calculation of the concentration of formate are slightly higher, ranging from 4.9 % to 5.9 %. Again, the experimental point at 120 min is the one which shows more variation respect to the model. These deviations of the model with respect to experiments are satisfactory since they are comparable to uncertainties in experimental results, reported in section3.1; indeed, inspection of Figs. 6 to 8 indicate that deviations can be attributed to a large extent to scatter of some

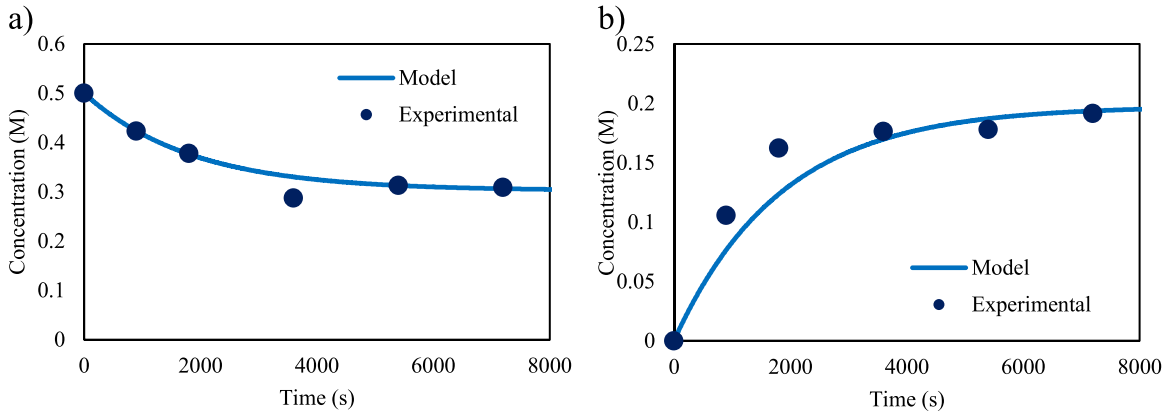

Fig. 6. Experimental data and modelization of the reaction kinetics at 200 °C. Reaction conditions: reactor filling: 40 %, reductant:CO_2 mole ratio: 5, Al powder as reductant and 0.018 g of Pd/C catalyst. a) $NaHCO_3$ decomposition kinetics and b) formate formation kinetics.

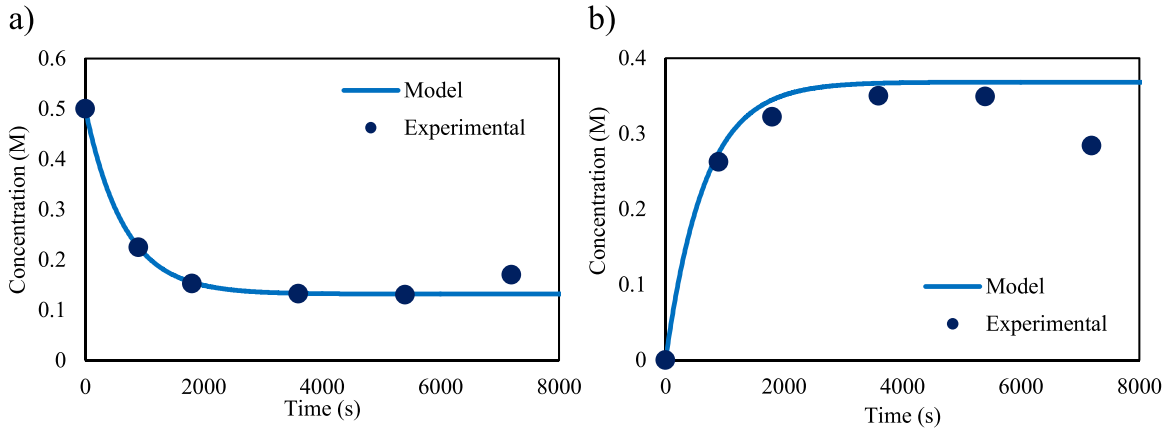

Fig. 7. Experimental data and modelization of the reaction kinetics at 250 °C. Reaction conditions: reactor filling: 40 %, reductant:CO_2 mole ratio: 5, Al powder as reductant and 0.018 g of Pd/C catalyst. a) $NaHCO_3$ decomposition kinetics and b) formate formation kinetics.

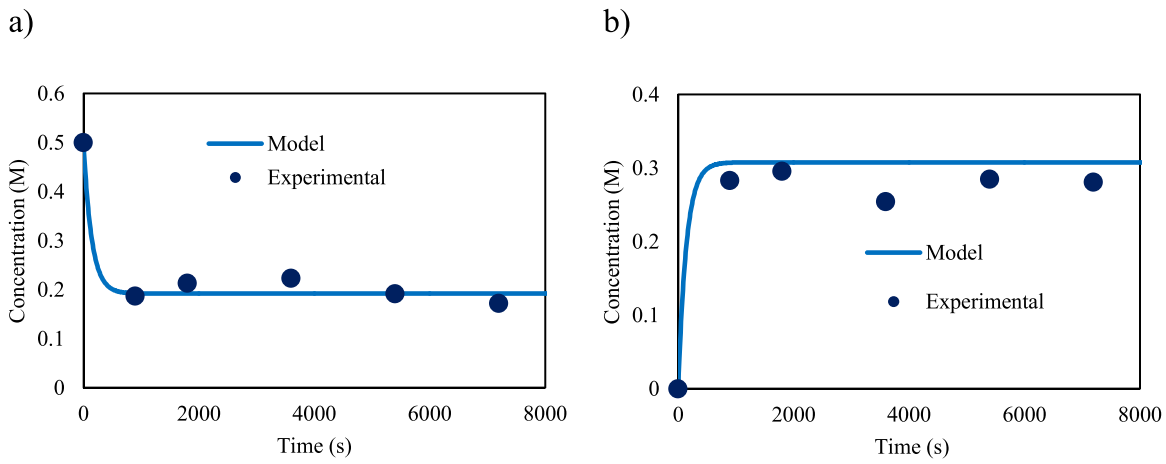

Fig. 8. Experimental data and modelization of the reaction kinetics at 300 ºC. Reaction conditions: reactor filling: 40 %, reductant:CO_2 mole ratio: 5, Al powder as reductant and 0.018 g of Pd/C catalyst. a) $NaHCO_3$ decomposition kinetics and b) formate formation kinetics.

Table 3
Value of the kinetic constants of bicarbonate decomposition and formate formation at different reaction temperatures.

Temperature (ºC)	k_1 (m^{-2} s^{-1})	k_2 (m^{-2} s^{-1})
200	0.034	$5.61 \cdot 10^{-3}$
250	0.162	$6.73 \cdot 10^{-3}$
300	1.352	$4.69 \cdot 10^{-2}$

experimental data, with the model correctly reproducing the global trends of variation of the results. Figs. 6 to 8 indicate that at least 95 % of the equilibrium concentration for both bicarbonate conversion and formate production are reached in the first 30 min of the reaction. Therefore, the reaction can be stopped after 30 min, reaching comparable yields with respect to 120 min reaction for this specific set of reaction parameters, this is, Pd/C catalyst and Al reductant at 250 ºC.

Table 3 summarizes the values of the kinetic constants, both for bicarbonate decomposition (k_1) and formate formation (k_2) at 200, 250 and 300 ºC. As one might expect, both kinetic constants increased at higher temperatures. The improvement observed from 250 to 300 ºC was more significant than from 200 to 250 ºC. Fig. 9.

The values of the activation energy (E_a/R) and the pre-exponential factor (A) calculated by Eq. 3 using the data obtained in Fig. 8 are shown in Table 4. The value of R^2 are also included.

The E_a for the formation of $HCOO^-$ from $NaHCO_3$ in hydrothermal media is 49.8 kJ/mol. The activation energy of the hydrogenation of CO_2 into formic acid over a $Cu/ZnO/Al_2O_3$ catalyst has been previously calculated resulting in a value of 21.4 kJ/mol [41]. Higher values of the activation energy indicate that the formation of the formate requires more energy input. Therefore, the formation of formate from $NaHCO_3$ under hydrothermal conditions needs more energy than when the production takes place by the hydrogenation of CO_2. The isothermal decomposition of $NaHCO_3$ into Na_2CO_3, CO_2 and H_2O presented an E_a of 94.3 kJ/mol [42] under nitrogen atmosphere which is a higher value in comparison to the decomposition of $NaHCO_3$ under hydrothermal calculated in this work which was 82.6 kJ/mol.

4. Conclusions

In this work, the hydrothermal conversion of CO_2 dissolved in aqueous solutions as $NaHCO_3$ was optimized at lower temperatures, with imply lower costs and milder conditions for the reuse of bases used for CO_2 capture, considering a number of combinations of reductants and catalysts, demonstrating the possibility of enhancing the yield to formate at lower temperatures by selecting the appropriate combination of reductant and catalyst. Moreover, the reductants and catalysts tested

Table 4
Values of E_a/R and pre-exponential factor (A) for the decomposition of $NaHCO_3$ and the formation of formate in the temperature range 200–300 ºC.

	E_a/R	A (m^{-2} s^{-1})	R^2
k_1	9937	$3.9 \cdot 10^{7}$	0.9805
k_2	5992	$5.7 \cdot 10^{2}$	0.7691

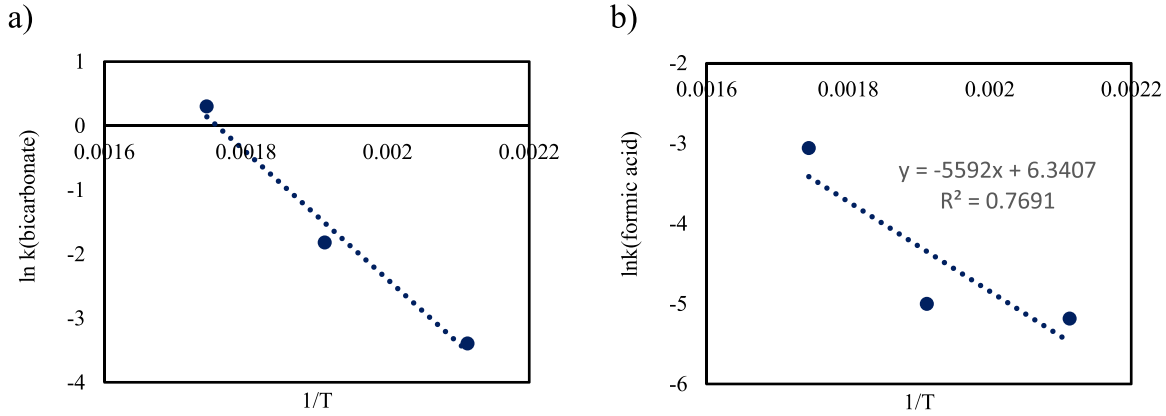

Fig. 9. Arrhenius plot for the hydrothermal reduction of $NaHCO_3$ into formate in the temperature range 200–300 ºC. Reaction conditions: reactor filling: 40 %, reductant:CO_2 mole ratio: 5, Al powder as reductant and 0.018 g of Pd/C catalyst. a) $NaHCO_3$ decomposition and b) formate formation.

are in general abundant and commercially available materials. The highest yield to formate observed was 57 % using Al as the reductant and Pd/C as the catalyst at 250 ºC. Using Al as reductant allowed to reach yields to formate higher than 50 % at 250 ºC. In the case of the other reductants tested (Zn and Fe), yields higher than 50 % were only observed when the temperature was 300 ºC. This improvement caused by the temperature was greater in the case of Fe reductant and Fe oxides catalysts, where the yields increased from 4 % at 250 ºC to 24 % and 31 % at 300 ºC for Fe_2O_3 and Fe_3O_4 respectively. Pd/C catalyst also showed higher yields to formate in comparison with the other catalysts tested at low temperatures with both Al and Zn reductants. In the case of Fe reductant, the yield with Pd/C was practically constant in the temperature range investigated.

Furthermore, a kinetic model was developed to describe the reduction of bicarbonate using Al as reductant and Pd as Catalyst. The simplified model model presents the system as a pseudo-equilibrium between formate formation and destruction. The model is able to reproduce the resulting concentrations, with average deviations with respect to experimental data ranging from 1.5 % to 5.9 %, and a maximum deviation lower than 10 %, and correctly predicts the variation of the performance of the reaction with the operating temperature.

The present study shows not only the potential of reducing CO_2 emissions by using it as a C1 building block, but also a sustainable alternative to produce value-added chemicals such as formic acid.

CRediT authorship contribution statement

Laura Quintana-Gómez: Methodology, Investigation, Writing – original draft. **Pablo Martínez-Álvarez:** Investigation. **José J. Segovia:** Conceptualization, Methodology. **Ángel Martín:** Conceptualization. Methodology. Resources. Writing – review & editing. Visualization. Supervision. Writing – review & editing. **María Dolores Bermejo:** Conceptualization, Methodology, Resources, Writing – Review & Editing, Supervision, Project administration, Funding acquisition.

Declaration of Competing Interest

The authors declare that they have no known competing financial interests or personal relationships that could have appeared to influence the work reported in this paper.

Data Availability

No data was used for the research described in the article.

Acknowledgments

This project has been funded by the Ministry of Science and Universities through project RTI2018-097456-B-I00 and by the Junta de Castilla y León through project by FEDER FUNDS under the BioEcoUVa Strategic Program (CLU-2019-04). Authors also thank Jesús Salvador Azpeleta Izquierdo (Universidad de Valladolid) for his support and assistance in XRD analysis and María Dolores Marqués Gutiérrez (Laboratorio de Sólidos Porosos Servicios Centrales de Apoyo a la Investigación –Universidad de Málaga) for her assistance in BET surface area analysis.

Appendix A. Supporting information

Supplementary data associated with this article can be found in the online version at doi:10.1016/j.jcou.2022.102369.

References

[1] K. Chang, H. Zhang, M.J. Cheng, Q. Lu, Application of ceria in CO_2 conversion catalysis, ACS Catal. 10 (2020) 613–631, https://doi.org/10.1021/acscatal.9b03935.
[2] CO2.earth. Monthly CO2 2021. https://www.co2.earth/monthly-co2 (accessed 9 May 2021).
[3] Z. Yuan, M.R. Eden, R. Gani, Toward the development and deployment of large-scale carbon dioxide capture and conversion processes, Ind. Eng. Chem. Res 55 (2016) 3383–3419, https://doi.org/10.1021/acs.iecr.5b03277.
[4] M.V. Landau, N. Meiri, N. Utsis, R. Vidruk Nehemya, M. Herskowitz, Conversion of CO_2, CO, and H2 in CO_2 hydrogenation to fungible liquid fuels on Fe-based catalysts, Ind. Eng. Chem. Res 56 (2017) 13334–13355, https://doi.org/10.1021/acs.iecr.7b01817.
[5] A. Yusuf, A. Giwa, E.O. Mohammed, O. Mohammed, A. Al Hajaj, M.R.M. Abu-Zahra, CO_2 utilization from power plant: a comparative techno-economic assessment of soda ash production and scrubbing by monoethanolamine, J. Clean. Prod. 237 (2019), 117760, https://doi.org/10.1016/j.jclepro.2019.117760.
[6] M. Yoo, S.J. Han, J.H. Wee, Carbon dioxide capture capacity of sodium hydroxide aqueous solution, J. Environ. Manag. 114 (2013) 512–519, https://doi.org/10.1016/j.jenvman.2012.10.061.
[7] Styring P., Jansen D., de Coninck H., Reith H., Armstrong K. Carbon Capture and Utilisation in the green economy. 2011.
[8] N.A.M. Razali, K.T. Lee, S. Bhatia, A.R. Mohamed, Heterogeneous catalysts for production of chemicals using carbon dioxide as raw material: a review, Renew. Sustain Energy Rev. 16 (2012) 4951–4964, https://doi.org/10.1016/j.rser.2012.04.012.
[9] H. Chen, H. Cui, Y. Lv, P. Liu, F. Hao, W. Xiong, et al., CO_2 hydrogenation to methanol over Cu/ZnO/ZrO2 catalysts: effects of ZnO morphology and oxygen vacancy, Fuel 314 (2022), 123035, https://doi.org/10.1016/j.fuel.2021.123035.
[10] L. Wan, X. Zhang, J. Cheng, R. Chen, L. Wu, J. Shi, et al., Bimetallic Cu-Zn catalysts for electrochemical CO2reduction: phase-separated versus core-shell distribution, ACS Catal. 12 (2022) 2741–2748, https://doi.org/10.1021/acscatal.1c05272.
[11] S. Zhang, X. Liu, Z. Shao, H. Wang, Y. Sun, Direct CO_2 hydrogenation to ethanol over supported Co2C catalysts: studies on support effects and mechanism, J. Catal. 382 (2020) 86–96, https://doi.org/10.1016/j.jcat.2019.11.038.
[12] C. He, G. Tian, Z. Liu, S. Feng, A mild hydrothermal route to fix carbon dioxide to simple carboxylic acids, Org. Lett. 12 (2010) 649–651, https://doi.org/10.1021/ol9025414.
[13] B. Michalkiewicz, Z.C. Koren, Zeolite membranes for hydrogen production from natural gas: state of the art, J. Porous Mater. 22 (2015) 635–646, https://doi.org/10.1007/s10934-015-9936-6.
[14] I.H.S. Markit. I.H.S. Markit: Production of Carbon-Free "Green" Hydrogen Could Be Cost Competitive by 2030 2020. https://news.ihsmarkit.com/prviewer/release_only/slug/bizwire-2020–7-15-ihs-markit-production-of-carbon-free-green-hydrogen-could-be-cost-competitive-by-2030 (accessed 1 June 2022).
[15] Z. Shen, Y. Zhang, F. Jin, The alcohol-mediated reduction of CO 2 and NaHCO 3 into formate: a hydrogen transfer reduction of NaHCO 3 with glycerine under alkaline hydrothermal conditions, RSC Adv. 2 (2012) 797–801, https://doi.org/10.1039/c1ra00886b.
[16] B. Jin, L. Luo, L. Xie, Pathways and kinetics for autocatalytic reduction of CO2into formic acid with Fe under hydrothermal conditions, ACS Omega 6 (2021) 11280–11285, https://doi.org/10.1021/acsomega.1c00119.
[17] Q. Fu, B. Sherwood Lollar, J. Horita, G. Lacrampe-Couloume, W.E. Seyfried, Abiotic formation of hydrocarbons under hydrothermal conditions: constraints from chemical and isotope data, Geochim Cosmochim. Acta 71 (2007) 1982–1998, https://doi.org/10.1016/j.gca.2007.01.022.
[18] T.M. McCollom, J.S. Seewald, A reassessment of the potential for reduction of dissolved CO_2 to hydrocarbons during serpentinization of olivine, Geochim Cosmochim. Acta 65 (2001) 3769–3778, https://doi.org/10.1016/S0016-7037(01)00655-X.
[19] D. He, X. Wang, Y. Yang, R. He, H. Zhong, Y. Wang, B. Han, F. Jin, Hydrothermal synthesis of long-chain hydrocarbons up to C24 with NaHCO3-assisted stabilizing cobalt, e2115059118, PRNAS 118 (51) (2021), https://doi.org/10.1073/pnas.2115059118.
[20] S.E. McGlynn, J.B. Glass, K. Johnson-Finn, F. Klein, S.A. Sanden, M.O. Schrenk, et al., Hydrogenation reactions of carbon on earth: linking methane, margarine, and life, Am. Miner. 105 (2020) 599–608, https://doi.org/10.2138/am-2020-6928CCBYNCND.
[21] C. Konn, J.L. Charlou, N.G. Holm, O. Mousis, The production of methane, hydrogen, and organic compounds in ultramafic-hosted hydrothermal vents of the mid-atlantic ridge, Astrobiology 15 (2015) 381–399, https://doi.org/10.1089/ast.2014.1198.
[22] X. Cui, F. Shi, Selective conversion of co2 by single-site catalysts, Wuli Huaxue Xuebao/ Acta Phys. - Chim. Sin. 37 (2021) 1–25, https://doi.org/10.3866/PKU.WHXB202006080.
[23] H. Zhong, G. Yao, X. Cui, P. Yan, X. Wang, F. Jin, Selective conversion of carbon dioxide into methane with a 98% yield on an in situ formed Ni nanoparticle catalyst in water, Chem. Eng. J. 357 (2019) 421–427, https://doi.org/10.1016/j.cej.2018.09.155.
[24] X. Wang, Y. Yang, T. Wang, H. Zhong, J. Cheng, F. Jin, In situ formed metal oxide /metal interface enhanced C-C coupling in CO_2 reduction into CH3COOH over hexagonal closed-packed cobalt, ACS Sustain. Chem. Eng. 9 (3) (2021) 1203–1212, https://doi.org/10.1021/acssuschemeng.0c06717.

[25] Z. Huo, M. Hu, X. Zeng, J. Yun, F. Jin, Catalytic reduction of carbon dioxide into methanol over copper under hydrothermal conditions, Catal. Today 194 (2012) 25–29, https://doi.org/10.1016/j.cattod.2012.06.013.
[26] J. Liu, X. Zeng, M. Cheng, J. Yun, Q. Li, Z. Jing, et al., Reduction of formic acid to methanol under hydrothermal conditions in the presence of Cu and Zn, Bioresour. Technol. 114 (2012) 658–662, https://doi.org/10.1016/j.biortech.2012.03.032.
[27] C. Jiang, H. Zhong, G. Yao, J. Duo, F. Jin, One-step water splitting and NaHCO3 reduction into hydrogen storage material of formate with Fe as the reductant under hydrothermal conditions, Int J. Hydrog. Energy 42 (2017) 17476–17487, https://doi.org/10.1016/j.ijhydene.2017.03.022.
[28] B. Wu, Y. Gao, F. Jin, J. Cao, Y. Du, Y. Zhang, Catalytic conversion of NaHCO3 into formic acid in mild hydrothermal conditions for CO_2 utilization, Catal. Today 148 (2009) 405–410, https://doi.org/10.1016/j.cattod.2009.08.012.
[29] H. Zhong, Y. Gao, G. Yao, X. Zeng, Q. Li, Z. Huo, et al., Highly efficient water splitting and carbon dioxide reduction into formic acid with iron and copper powder, Chem. Eng. J. 280 (2015) 215–221, https://doi.org/10.1016/j.cej.2015.05.098.
[30] J. Duo, F. Jin, Y. Wang, H. Zhong, L. Lyu, G. Yao, et al., NaHCO3-enhanced hydrogen production from water with Fe and in situ highly efficient and autocatalytic NaHCO3 reduction into formic acid, Chem. Commun. 52 (2016) 3316–3319, https://doi.org/10.1039/c5cc09611a.
[31] X. Zeng, M. Hatakeyama, K. Ogata, J. Liu, Y. Wang, Q. Gao, et al., New insights into highly efficient reduction of CO_2 to formic acid by using zinc under mild hydrothermal conditions: A joint experimental and theoretical study, Phys. Chem. Chem. Phys. 16 (2014) 19836–19840, https://doi.org/10.1039/c4cp03388d.
[32] F. Jin, X. Zeng, J. Liu, Y. Jin, L. Wang, H. Zhong, et al., Highly efficient and autocatalytic H2O dissociation for CO_2 reduction into formic acid with zinc, Sci. Rep. 4 (2014) 1–8, https://doi.org/10.1038/srep04503.
[33] H. Zhong, L. Wang, Y. Yang, R. He, Z. Jing, F. Jin, Ni and Zn/ZnO synergistically catalyzed reduction of bicarbonate into formate with water splitting, ACS Appl. Mater. Interfaces 11 (45) (2019) 42149–42155, https://doi.org/10.1021/acsami.9b14039.
[34] G. Yao, X. Zeng, Y. Jin, H. Zhong, J. Duo, F. Jin, Hydrogen production by water splitting with Al and in-situ reduction of CO_2 into formic acid, Int J. Hydrog. Energy 40 (2015) 14284–14289, https://doi.org/10.1016/j.ijhydene.2015.04.073.
[35] D. Roman-Gonzalez, A. Moro, F. Burgoa, E. Pérez, A. Nieto-Márquez, Á. Martín, et al., Hydrothermal CO_2 conversion using zinc as reductant: Batch reaction, modeling and parametric analysis of the process, J. Supercrit. Fluids 140 (2018) 320–328, https://doi.org/10.1016/j.supflu.2018.07.003.
[36] J. Yu, P.E. Savage, Decomposition of formic acid under hydrothermal conditions, Ind. Eng. Chem. Res 37 (1998) 2–10, https://doi.org/10.1021/ie970182e.
[37] S. Horstmann, A. Jabłoniec, J. Krafczyk, K. Fischer, J. Gmehling, PSRK group contribution equation of state: comprehensive revision and extension IV, including critical constants and α-function parameters for 1000 components, Fluid Phase Equilib. 227 (2005) 157–164, https://doi.org/10.1016/j.fluid.2004.11.002.
[38] W. Wagner, A. Pruß, The IAPWS formulation 1995 for the thermodynamic properties of ordinary water substance for general and scientific use, J. Phys. Chem. Ref. Data 31 (2002) 387–535, https://doi.org/10.1063/1.1461829.
[39] Y. Le, H. Zhong, Y. Yang, R. He, G. Yao, F. Jin, Mechanism study of reduction of CO_2 into formic acid by in-situ hydrogen produced from water splitting with Zn: Zn/ZnO interface autocatalytic role, J. Energy Chem. 26 (2017) 936–941, https://doi.org/10.1016/j.jechem.2017.03.013.
[40] RRUFF project, https://rruff.info, retrieved on November 2022.
[41] C.L. Chiang, K.S. Lin, H.W. Chuang, Direct synthesis of formic acid via CO_2 hydrogenation over Cu/ZnO/Al2O3 catalyst, J. Clean. Prod. 172 (2018) 1957–1977, https://doi.org/10.1016/j.jclepro.2017.11.229.
[42] B. Janković, Kinetic analysis of isothermal decomposition process of sodium bicarbonate using the weibull probability function-estimation of density distribution functions of the apparent activation energies, Met. Mater. Trans. B Process Met. Mater. Process Sci. 40 (2009) 712–726, https://doi.org/10.1007/s11663-009-9271-x.